Predicting the dependency of a degree of saturation on void ratio and suction using effective stress principle for unsaturated soils

David Mašín

Charles University

Faculty of Science

Institute of Hydrogeology, Engineering Geology and Applied Geophysics

Albertov 6

12843 Prague 2, Czech Republic

E-mail: masin@natur.cuni.cz

Tel: +420-2-2195 1552, Fax: +420-2-2195 1556

March 31, 2009

Revised version of a paper considered for publication in IJNAMG

Abstract

The paper presents an approach to predicting variation of a degree of saturation in unsaturated soils with void ratio and suction. The approach is based on the effective stress principle for unsaturated soils and several underlying assumptions. It focuses on the main drying and wetting processes and does not incorporate the effects of hydraulic hysteresis. It leads to the dependency of WRC on void ratio, which does not require any material parameters apart from the parameters specifying WRC for the reference void ratio. Its validity is demonstrated by comparing predictions with experimental data on four different soils taken over from the literature. Good correlation between the measured and predicted behaviour indirectly supports applicability of the effective stress principle for unsaturated soils.

Keywords: Unsaturated soils; effective stress; water retention curve

1 Introduction

The degree of saturation S_r in unsaturated soils depends on partial pressures of water and air phase (measured by matric suction s) and on void ratio. The dependency of S_r on s is described by a water retention curve (WRC, also denoted as a soil water characteristic curve). The WRC itself is, due to the dependency of S_r on e, void ratio dependent.

Constitutive models for hydraulic behaviour of unsaturated soils may be broadly divided into two groups. Models from the first group take advantage of the fact that the influence of s on S_r is more significant than the influence of e and they neglect the influence of volumetric deformations on S_r. In general, these models are more common in the literature on unsaturated soil behaviour (for example [32, 18, 34]) than models of the second group that take the dependency of WRC on e into account.

Models of the first group indeed fail in predicting variation of S_r in experiments where the soil undergoes substantial volumetric deformation. To overcome this limitation, several models were proposed, notable examples are Sun et. al [30, 31], Gallipoli et al. [6] and Nuth and Laloui [25]. In these models, a unique dependency of the water retention curve on void ratio is considered, which yields a state surface in the S_r vs. s vs. e space unique for the main drying and main wetting process. In the cited papers, the dependency of S_r on e and s is controlled by an empirical formulation, and additional soil parameters are typically needed in order to characterise the dependency of WRC on e. The state surface described may be seen as an advance from the

early concept of state surface by Matyas and Radhakrishna [22] and Lloret and Alonso [19], who considered a unique relationship between S_r, s and a mean net stress p_{net}.

In this paper, a new approach to evaluation of the dependency of WRC on e is presented. This approach is based on several underlying principles derived in [15, 20] and leads to the dependency of WRC on e, which is not controlled by additional model parameters. This property is desirable for practical application of coupled hydro-mechanical models for unsaturated soils.

The paper is organised as follows: Basic assumptions for the present developments are summarised in Sec. 2. These consist of selection of stress state variables and formulation of WRC for constant void ratio. An approach relating the dependency of S_r on volumetric deformation, derived by Loret and Khalili [20], is then presented in Sec. 3. Sec. 4 gives additional motivations for the present work and demonstrates some limitations of existing formulations. Quantification of the dependency of S_r on e and s is then given in Sec. 5. Sec. 6 summarises determination of new material parameters. Finally, the proposed approach is evaluated in Sec. 7 using experimental data on different soils taken over from literature.

Notation: Following the sign convention of continuum mechanics compression is taken as negative throughout this paper. However, variables p (mean stress), ϵ_v (volumetric strain) and suction $s = -(u_a - u_w)$ are defined to be positive in compression.

2 Adopted descriptions of the stress state and water retention curve

2.1 Stress state description

Applicability of the effective stress principle for unsaturated soils is a matter of decades lasting discussions. Currently, it is generally accepted that two stress variables are needed for proper description of the stress state within unsaturated soil. In addition to the tensorial stress variable, the second (typically scalar) variable is needed to describe stiffening effect of water menisci on the soil structure (in the context of critical state soil mechanics, it controls the size of state boundary surface). If the first variable combines the influence of total stress and pore fluids in such a way that it describes their effect on volumetric and shear behaviour of overconsoildated soils, it can be seen as an equivalent to the effective stress in saturated soils. In this paper, following [15, 20], this variable will be denoted as effective stress, although it is recognised that different terms are

suggested by different authors (such as average skeleton stress [5] or intergranular stress [11]).

The effective stress in unsaturated soils $\boldsymbol{\sigma}'$ may be in general written as

$$\boldsymbol{\sigma}' = \boldsymbol{\sigma} - \chi u_w \mathbf{1} - (1-\chi) u_a \mathbf{1} = \boldsymbol{\sigma}_{net} - \chi s \mathbf{1} \tag{1}$$

where $\boldsymbol{\sigma}$ is a total stress, u_a is the pore air pressure and u_w is the pore water pressure, $\boldsymbol{\sigma}_{net}$ is the net stress defined as $\boldsymbol{\sigma}_{net} = \boldsymbol{\sigma} - u_a \mathbf{1}$ and s is matric suction $s = -(u_a - u_w)$. χ is the Bishop [1] effective stress factor. The incremental form of (1) is written as

$$\dot{\boldsymbol{\sigma}}' = \dot{\boldsymbol{\sigma}} - \psi \dot{u}_w \mathbf{1} - (1-\psi)\dot{u}_a = \boldsymbol{\sigma}_{net} - \psi \dot{s} \mathbf{1} \tag{2}$$

where

$$\psi = \frac{d(\chi s)}{ds} \tag{3}$$

The effective stress factor χ from Eq. (1) specifies the relative contribution of the pore air and water pressures to the effective stress.

Gens and Gens et al. [7, 8] proposed classification of the tensorial stress variable according to variables incorporated in the formulation of χ: class 1 considers $\chi = 0$, class 2 makes χ a function of suction and class 3 incorporates s and S_r into the definition of χ. Class 2 and class 3 formulations may take particular forms that satisfy the definition of the effective stress in unsaturated soils; class 1 formulation is a net stress and as such it is out of the scope of this paper. For a detailed review of different formulations proposed in the literature the reader is referred to [8, 25].

Class 3 formulations are popular in the literature on unsaturated soil modelling thanks to their conceptual advantages, such as straightforward transition between saturated and unsaturated states and direct incorporation of a hydraulic hysteresis. To this class belongs the classic form due to Bishop [1], who proposed $\chi = S_r$ using a phenomenological approach. The same formulation was subsequently derived from different theoretical considerations in [9, 16, 17, 10] and it was used in many constitutive models for unsaturated soils [35, 5, 2, 32]. Note that although the assumption of $\chi = S_r$ is often used thanks to its convenience, its validity has actually not been proved experimentally (e.g., Jennings and Burland [11]).

In class 2 models, χ is considered solely a function of matric suction. Among advantages of the class 2 models belongs the fact that it is possible to represent stress state also in the case when

data on water content are not available or are unreliable. A suitable empirical expression, which was shown to be capable of predicting both volume changes and shear strength behaviour of unsaturated soils, was proposed by Khalili and Khabbaz [15] and Khalili et al. [13]. They have related the factor χ to suction and to the suction at the transition between saturated and unsaturated states s_e by

$$\chi = \begin{cases} 1 & \text{for} \quad s < s_e \\ \left(\frac{s_e}{s}\right)^{\gamma} & \text{for} \quad s \geq s_e \end{cases} \tag{4}$$

Eq. (4) does not consider hydraulic hysteresis. This means it is applicable only for states which are on the main drying branch of WRC for constant or increasing suction (then s_e equal to the air-entry value of suction), or on the main wetting branch of WRC for constant or decreasing suction (then s_e equal to the air-expulsion value of suction). A possible way to incorporate the effects of hydraulic hysteresis has been proposed by Khalili et al. [14]. Khalili and Khabbaz [15] have shown that the best-fit value of the exponent $\gamma = 0.55$ is suitable to represent the behaviour of different soil types. γ can therefore be considered as a material independent constant. s_e depends on the soil type and on the void ratio, though in the original formulation it is for simplicity considered as constant.

Eq. (4) leads using (3) to the following expression for the incremental effective stress factor ψ:

$$\psi = \begin{cases} 1 & \text{for} \quad s < s_e \\ (1-\gamma)\chi & \text{for} \quad s \geq s_e \end{cases} \tag{5}$$

The effective stress formulation from Eq. (4) has already been applied in many constitutive models for unsaturated soils (e.g., [14, 21, 20, 23, 24, 26]). It will be used as a basis for developments presented in this paper.

2.2 Water retention curve

Unlike the exponent γ of the effective stress factor χ in (4), the degree of saturation S_r vs. suction relationship (i.e., WRC) for a given void ratio depends significantly on the soil type and the granulometry (e.g., Ref. [4]). Many different mathematical relationships for the WRC with variable complexity are available throughout the literature [3, 14, 18, 34]. In this paper, a simple

formulation formally similar to that by Brooks and Corey [3] will be used:

$$S_r = \begin{cases} 1 & \text{for} \quad s < s_e \\ \left(\frac{s_e}{s}\right)^{\lambda_p} & \text{for} \quad s \geq s_e \end{cases} \tag{6}$$

valid for $S_r > S_{res}$, where S_{res} is the residual degree of saturation. s_e is the air-entry or air-expulsion suction as in Eq. (4). Similarly to the adopted expression for the effective stress factor χ, Eq. (6) neglects the effects of hydraulic hysteresis. It may therefore be considered as appropriate for representation of the main drying and wetting branches of the WRC. In (6), both factors s_e and λ_p depend on the soil type and on void ratio.

3 Basic relations between volume changes and effective stress in unsaturated soils

Considering the existence of generalised elastic and plastic potentials, Loret and Khalili [20] and Khalili et. al [14] derived the following constitutive formulations for the pore water volume (V_w) and pore air volume (V_a) changes:

$$-\frac{\dot{V}_w}{V} = \psi\dot{\epsilon_v} - a_{11}\dot{u}_w - a_{12}\dot{u}_a \tag{7}$$

$$-\frac{\dot{V}_a}{V} = (1-\psi)\dot{\epsilon_v} - a_{21}\dot{u}_w - a_{22}\dot{u}_a \tag{8}$$

in which V is total volume of a soil element, $\dot{\epsilon}_v = -\dot{V}/V$ is the rate of soil skeleton volumetric strain, a_{ij} are material parameters and ψ is the effective stress rate factor from Eq. (5). They can be determined from the water retention curve defined in terms of degree of saturation $S_r = V_w/V_v$, with V_v being volume of voids. The definition of S_r implies

$$\dot{V}_w = S_r\dot{V}_v + \dot{S}_r V_v \tag{9}$$

and therefore

$$\frac{\dot{V}_w}{V} = -S_r\dot{\epsilon}_v + n\dot{S}_r \tag{10}$$

$n = V_v/V$ is porosity, the degree of saturation S_r depends on suction s, void ratio and on the suction-loading path. We may therefore write

$$\dot{S}_r = \frac{\partial S_r}{\partial s}\dot{s} + \frac{\partial S_r}{\partial \epsilon_v}\dot{\epsilon}_v \tag{11}$$

which can be substituted into (10):

$$\frac{\dot{V}_w}{V} = -\left(S_r - n\frac{\partial S_r}{\partial \epsilon_v}\right)\dot{\epsilon}_v + n\frac{\partial S_r}{\partial s}\dot{s} \tag{12}$$

Comparing (12) with (7) we have

$$\psi = S_r - n\frac{\partial S_r}{\partial \epsilon_v} = S_r + e\frac{\partial S_r}{\partial e} \tag{13}$$

where $e = n/(1-n)$ is void ratio. Substituting (13) into (11) yields the following general expression for the rate of the degree of saturation S_r:

$$\dot{S}_r = \frac{\partial S_r}{\partial s}\dot{s} + \frac{\psi - S_r}{e}\dot{e} \tag{14}$$

The first term in (14) quantifies the dependency of S_r on suction at constant void ratio (i.e., water retention curve at constant void ratio), and the second term evaluates the dependency of S_r on void ratio at constant suction. Eq. (14) was originally derived by Khalili et al. in [20, 14].

4 Additional motivation for the present work

Eq. (14) can be used to calculate a rate of the degree of saturation from rates of void ratio and suction. In the following it is shown that using the rate form for calculation of changes of S_r with s and e (Eq. (14)) in combination with the effective stress formulation of Eq. (4) with constant s_e, and WRC formulation of Eq (6) with constant λ_p, leads to incorrect results.

Consider two specimens of the same void ratio e_0 and air-expulsion suction s_{e0} at two different suction levels, shown in Fig. 1a. Both the two specimens lie on a single wetting branch of a water retention curve corresponding to e_0 (states A and B). The specimens are first subject to a void ratio increase at constant suction to a void ratio e_1 (paths A-A' and B-B'), followed by a suction decrease at constant void ratio e_1 up to a full saturation (paths A'-A" and B'-B").

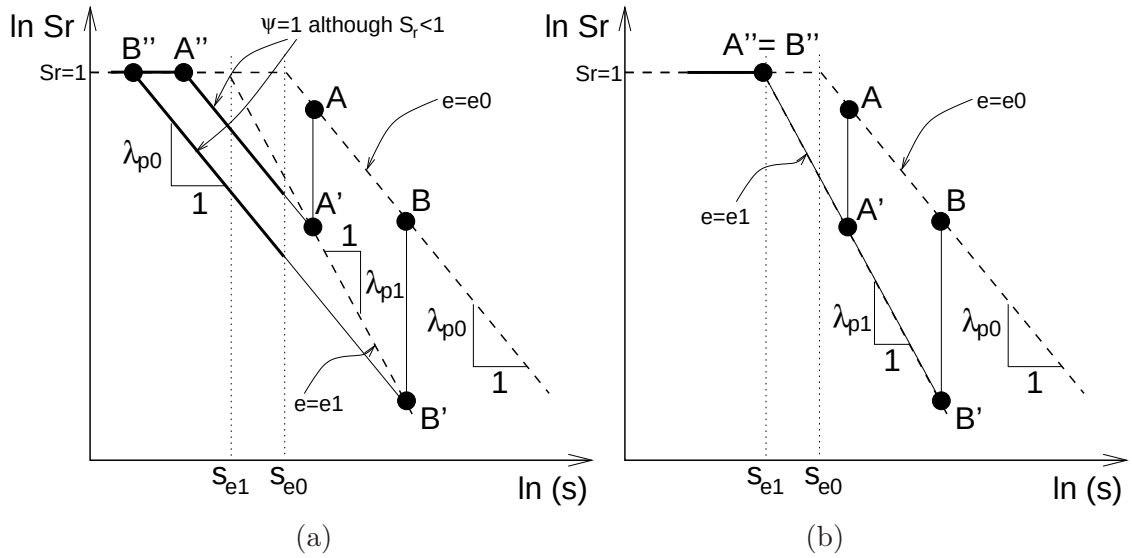

Figure 1: Theoretical experiment demonstrating motivation for the present work. (a) response by Eq. (14) without e-dependent s_e and λ_p; (b) response by the proposed model.

In the following it is *assumed* that the main drying and main wetting branches of WRC are only dependent on void ratio and independent on the stress history. Based on this assumption, the two paths A'-A" and B'-B" should lie on the same wetting branch of WRC corresponding to the void ratio e_1, as shown in Fig. 1b. Instead, direct application of Eq. (14) for calculation of changes of S_r with constant λ_p predicts that the two specimens follow different paths in S_r vs. s plane during suction decrease (Fig. 1a). The anticipated response may be obtained if void ratio dependent value of λ_p is considered. Note that Fig. 1b presumes $\lambda_{p1} > \lambda_{p0}$ for $e_1 > e_0$. This dependency is implied by derivations presented subsequently in Sec. 5.

In addition to the problems described above, application of the effective stress principle from [15] with constant air-expulsion value s_{e0}, with the factor ψ defined as in Eq. (5), imposes incorrectly $\psi = 1$ for all states with $s < s_{e0}$, therefore also for states with $S_r < 1$ (Fig. 1a). This problem may be overcome in two ways. First, e-dependency of s_e may be considered. A suitable relationship is derived in Sec. 5. Second, the effective stress factor χ from Eq. (4) may be, considering the adopted formulation for WRC (6), equivalently expressed in terms of S_r

$$\chi = S_r^{(\gamma/\lambda_p)} \tag{15}$$

The effective stress rate factor reads $\psi = d(\chi s)/ds$, after substitution of Eqs. (15) and (6) we

therefore have

$$\psi = S_r^{(\gamma/\lambda_p)} + s\frac{dS_r^{(\gamma/\lambda_p)}}{ds} = (1-\gamma)S_r^{(\gamma/\lambda_p)} = (1-\gamma)\chi \tag{16}$$

Using straightforward transformation of Eqs. (15) and (16), the class 2 effective stress expression is directly converted into class 3 formulation. Definition of χ in terms of S_r by Eq. (15) eliminates s_e from the effective stress equation. This transformation is indeed valid for the main wetting and drying branches of WRC, provided that the double-logarithmic expression for WRC (6) is considered as appropriate. More research would be needed to study whether it is applicable also in the cases in which the effects of hydraulic hysteresis are important.

5 Quantification of the dependency of S_r on suction and void ratio

In this section, solution to problems outlined in Sec. 4 is presented. The derivations are applicable for an unsaturated state, where $s \geq s_e$ and therefore $\psi = (1-\gamma)\chi$. They are detailed in Appendix. It is shown that the rate of the suction at air entry/expulsion s_e can be calculated by

$$\dot{s}_e = -\frac{\gamma s_e}{e\lambda_{psu}}\dot{e} \tag{17}$$

with

$$\lambda_{psu} = \frac{\gamma}{\ln\chi_{0su}} \ln\left[\left(\chi_{0su}^{\frac{\lambda_{p0}}{\gamma}} - \chi_{0su}\right)\left(\frac{e}{e_0}\right)^{(\gamma-1)} + \chi_{0su}\right] \tag{18}$$

where $\chi_{0su} = (s_{e0}/s_e)^\gamma$. s_{e0} and λ_{p0} are values of s_e and λ_p corresponding to the reference void ratio e_0. Dependency of λ_p on void ratio and suction is given by

$$\lambda_p = \frac{\gamma}{\ln\chi_0} \ln\left[\left(\chi_0^{\frac{\lambda_{p0}}{\gamma}} - \chi_0\right)\left(\frac{e}{e_0}\right)^{(\gamma-1)} + \chi_0\right] \tag{19}$$

with $\chi_0 = (s_{e0}/s)^\gamma$.

Knowledge of s_e from (19) and λ_p from (18) may be used to calculate the value of S_r for given void ratio and suction using Eq. (6). Eqs. (17-19) describe a state surface in the s vs. e vs. S_r space, which is depicted in Fig. 2 for Pearl clay parameters from Tab. 1. Constant-void-ratio

cross-sections through this surface represent water retention curves, shown in Fig. 3a. Figs. 2 and 3a also demonstrate how increasing void ratio leads to the decrease of the s_e value. Figure 3b shows the influence of e and s on the slope λ_p of the WRC.

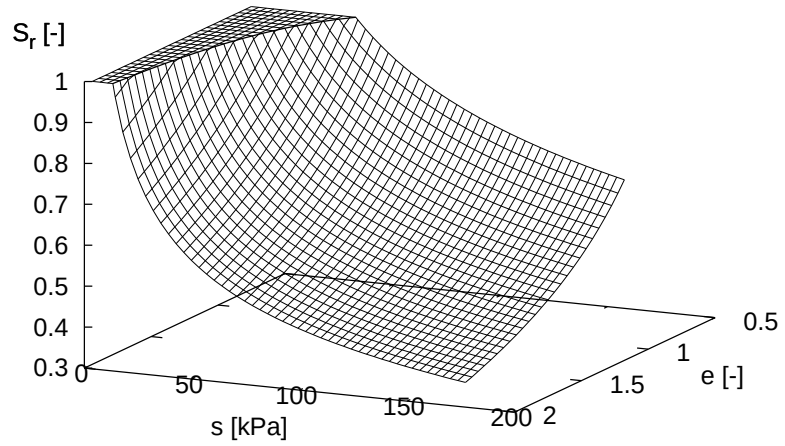

Figure 2: Predicted state surface in the s vs. e vs. S_r space.

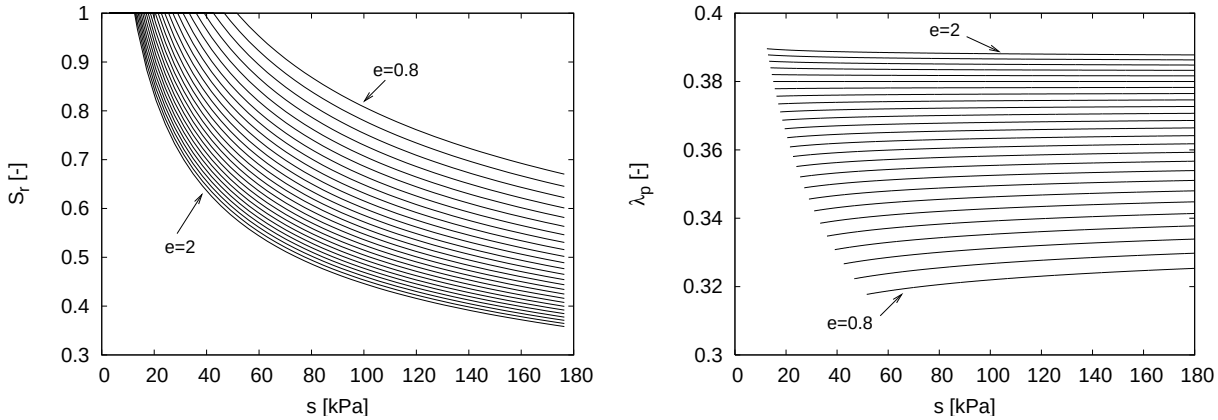

(a) (b)

Figure 3: (a) dependency of WRC on void ratio; (b) dependency of the slope λ_p of the WRC on s and e for reference values $\lambda_{p0} = 0.38$, $s_{e0} = 15$ kPa and $e_0 = 1.75$.

Two ways may be followed in the case the rate form of S_r is required (Eq. (14)). The derivative $\partial S_r/\partial s$ may either be found numerically from (6), or it can be substituted by $-\lambda_p S_r/s$ if the dependency of λ_p on s is neglected. This dependency is not significant for void ratios not significantly different as compared to the reference void ratio e_0 (see Fig. 3b).

Note that the derivations presented in this section include the Bishop effective stress factor χ equal to S_r as a special case. In this case $\lambda_{p0} = \gamma$ and Eq. (19) simplifies to $\lambda_p = \lambda_{p0}$ (i.e., λ_p is

independent of suction and of void ratio). The Equation (17) may then be integrated analytically, with resulting $s_e = s_{e0} e_0 / e$.

6 Determination of parameters

The model requires three material parameters. Parameters s_{e0} and λ_{p0} may be found directly by bi-linear representation of the water retention curve in the $\ln S_r$ vs. $\ln(s/s_{e0})$ plane, as shown in Fig. 4. Parameter e_0 is void ratio corresponding to the approximated WRC.

Alternatively, the parameters may be found by a trial-and-error procedure using S_r vs. s vs. e data coming from laboratory experiments. In principle, any experiment with monotonous path may be used for this purpose. For example compression or shear tests at constant suction, wetting/drying tests at constant net stress, constant water content experiments, etc. Note that the value of e_0 may be selected arbitrarily to be in the range of reasonable void ratios for the given soil. The calibration using the trial-and-error procedure is demonstrated in Fig. 4b, which shows p_{net} vs. S_r diagram of constant suction isotropic loading-unloading test on bentonite/kaolin mixture by Sharma [27] and predictions with the proposed model with $e_0 = 1.2$ and variable s_{e0} and λ_{p0}. Note that only one test is shown in Fig. 4b for clarity. Proper calibration using the trial-and-error procedure requires considering more tests with variable suction and/or void ratio.

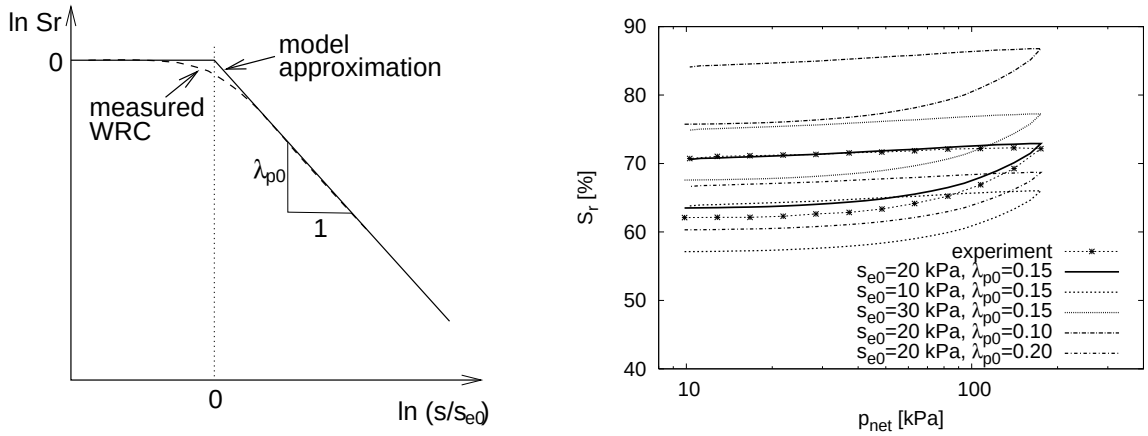

(a) (b)

Figure 4: (a) Direct determination of parameters s_{e0}, λ_{p0} and e_0 by a bi-linear representation of the WRC; (b) calibration by the trial-and-error procedure using S_r vs. s vs. e data (experimental data by Sharma, 1995).

7 Comparison with experimental data

The proposed dependency of WRC on void ratio will be in the following evaluated with respect to a wide range of different soils. All predictions presented are obtained using Eqs. (17-19). The predicted degree of saturation S_r is calculated directly from the experimentally measured e and s without a need to couple the present hydraulic model with a mechanical constitutive model for partly saturated soils. Parameters used in the present evaluation are summarised in Tab. 1.

It is interesting to note that for all studied soils the value of λ_{p0} is significantly lower than $\gamma = 0.55$, demonstrating empirically that the popular assumption of $\chi = S_r$ would not lead to accurate predictions, even if the dependency of s_e on e as discussed above would have been taken into account.

Table 1: Parameters of the proposed formulation used in the present evaluation.

soil	s_{e0} [kPa]	λ_{p0} [-]	e_0 [-]
Pearl clay	15	0.38	1.75
HPF quartz silt	3	0.18	0.7
Speswhite kaolin	65	0.3	1.4
bentonite/kaolin mix.	20	0.15	1.2

7.1 Pearl clay

Sun et al. [28, 31, 29] presented results of isotropic compression and wetting tests on statically compacted Pearl clay, which is a moderate plasticity soil with very little expansive clay minerals, containing quartz, pyrophyllite and kaolinite in the order of dominance. Figure 5 shows results of isotropic compression tests at constant suction $s = 147$ kPa. The four tests, which started at different void ratios (Fig. 5a), were used for calibration of model parameters using the trial-end-error procedure. The degree of saturation predicted by the proposed formulation is in a reasonable agreement with the experimental results (Figures 5b,c).

In the second set of experiments, isotropic compression tests at constant suction of 147 kPa starting from the same initial void ratio were followed by wetting at different mean net stress levels. The p_{net} vs. e relationships are given in Fig. 6. The degrees of saturation in the tests were predicted using parameter values obtained from constant suction compression tests from Fig. 5. Experimental results in Figs. 6b,c show predictions in the p_{net} vs. S_r plane, Figs. 6d,e in s vs. S_r plane. The predictions are in a reasonable agreement with the experiments, even though the

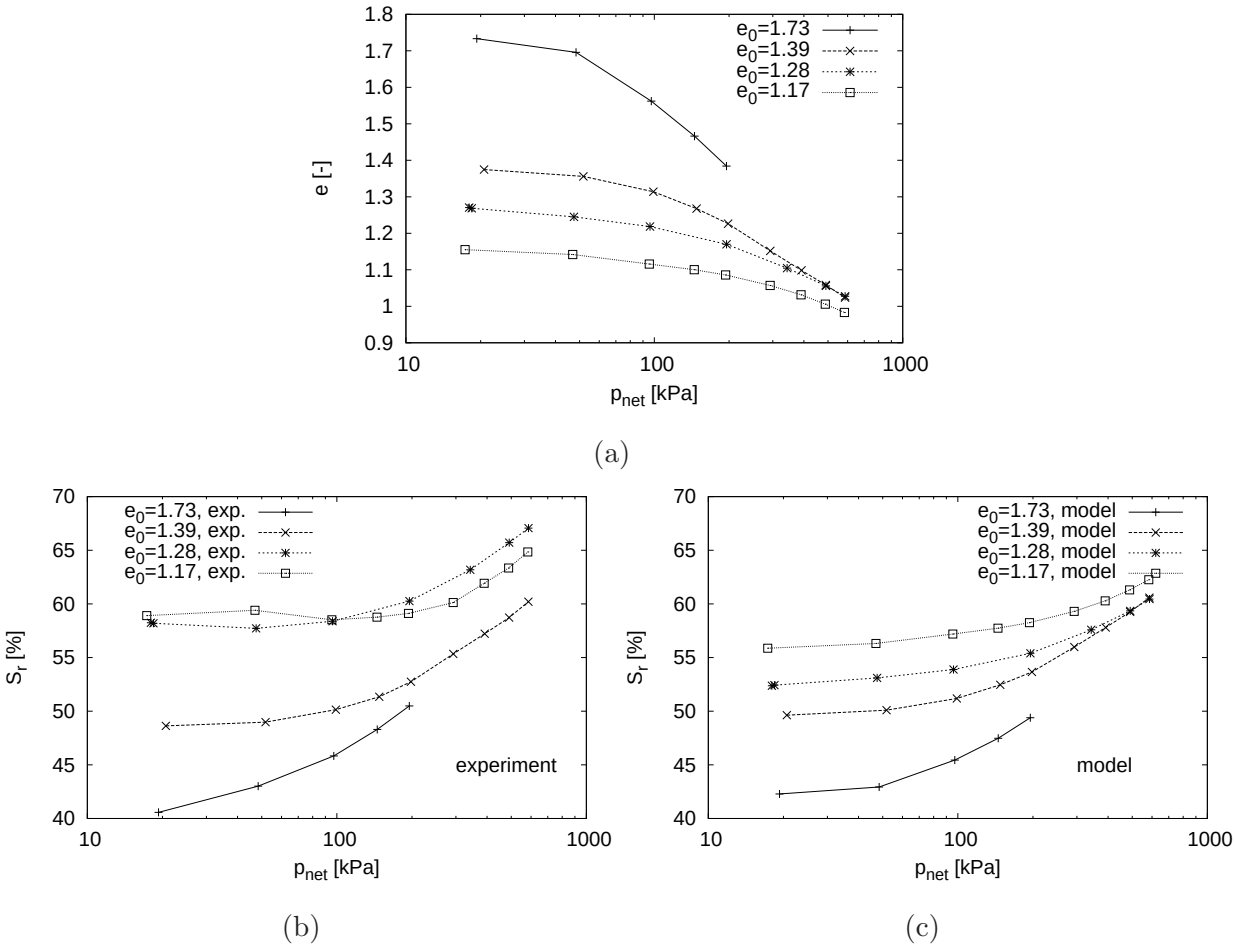

Figure 5: Constant suction isotropic compression tests at different initial void ratios by Sun et al. [31]. (a) measured void ratios, (b) measured S_r, (c) predicted S_r.

parameters were calibrated using compression tests at constant suction.

7.2 HPF quartz silt

Jotisankasa et. al [12] performed a set of constant water content oedometric tests with monitored suction on a mixture of 70 % silt of HPF type (consisting mainly of angular quartz grains), 10% kaolin and 20% London clay. The authors made available the WRC measured by standard filter paper technique at zero vertical stress, which allows us to calibrate the proposed model using the direct approach, which has been demonstrated in Fig. 4a. Figure 7 shows the wetting branch of the WRC starting from compacted state at $s = 1000$ kPa and void ratio $e_0 = 0.7$. Figure 7 also shows the WRC predicted by the proposed model with $e_0 = 0.7$, $s_{e0} = 3$ kPa and variable λ_{p0}. The model curve for $\lambda_{p0} = 0.18$ reproduces well the experimental data, demonstrating suitability of Eq. (6) for the present purpose.

The oedometric tests by Jotisankasa et. al [12] were performed at constant water content

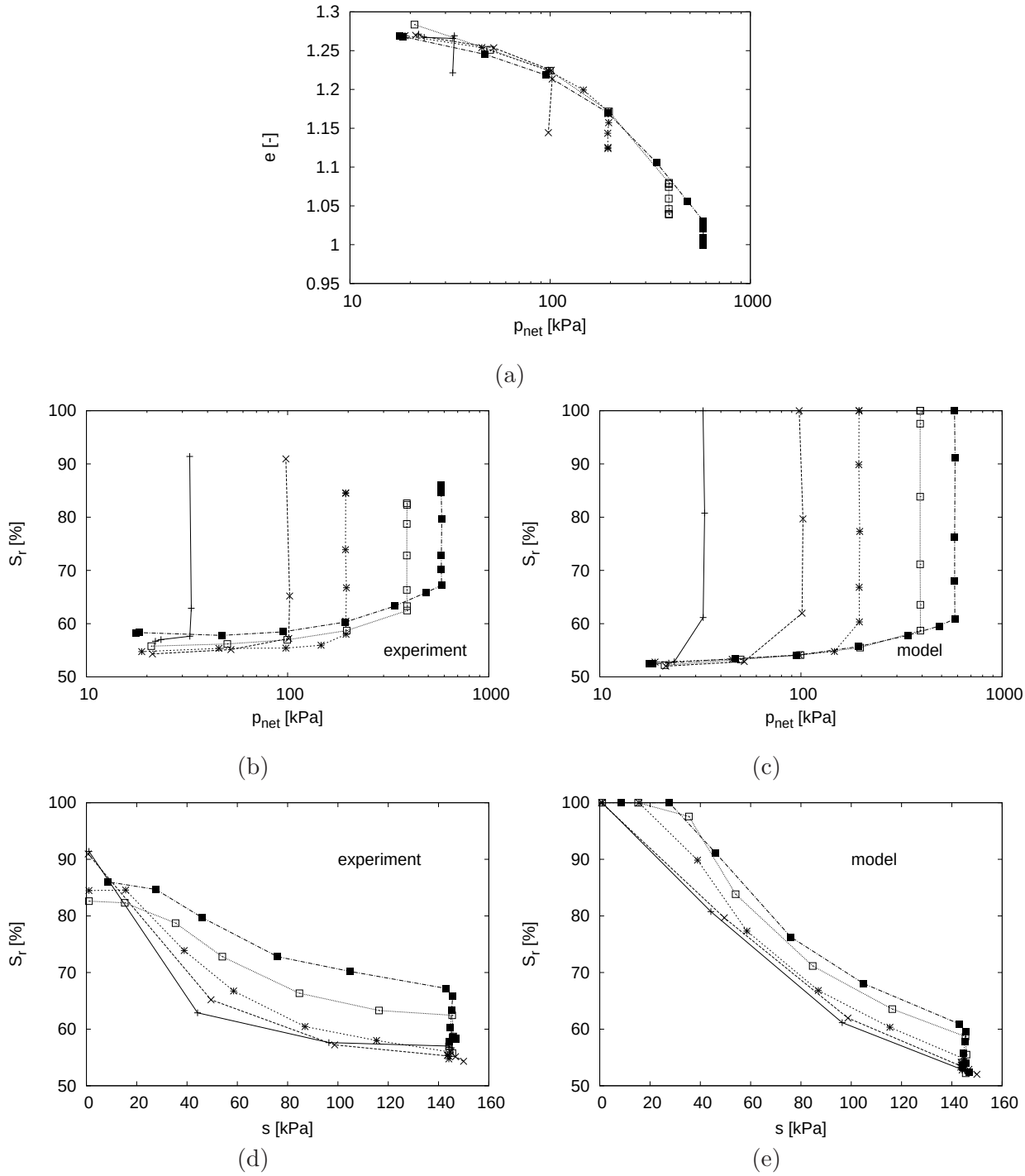

Figure 6: Constant suction isotropic compression tests and wetting tests at different mean net stress levels by Sun et al. [31]. (a) measured void ratios, (b-e) experimental and simulated S_r.

conditions, therefore both suction and void ratio varied during compression. Figures 8a,b and c show the measured dependencies of void ratio, suction and degree of saturation for five different tests. The tests were modeled using the proposed approach with soil parameters obtained using direct calibration from WRC (Fig. 7). The predictions are shown in Fig. 8b. The model is in a perfect match with the experiments, although tests with variable void ratio were not involved in

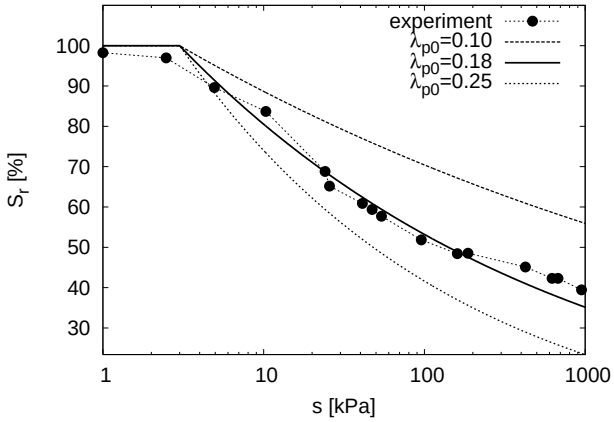

Figure 7: wetting branch of WRC of HPF type quartz silt, experimental data by Jotisankasa et. al (2007), direct calibration of the proposed model with $e_0 = 0.7$, $s_{e0} = 3$ kPa and variable λ_{p0}.

model calibration.

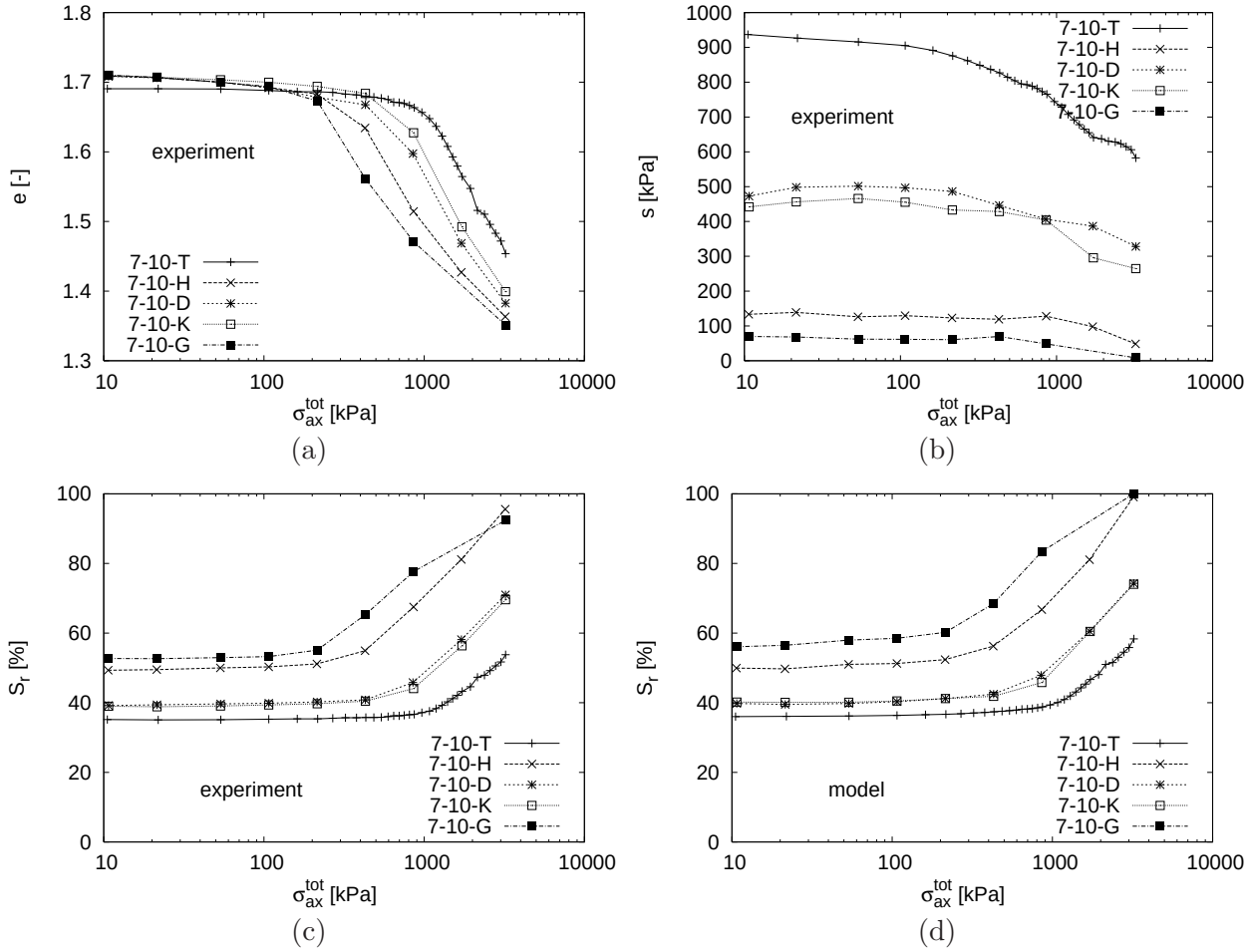

Figure 8: Results of suction-monitored oedometric tests at constant water content by Jotisankasa et. al (2007) (a,b,c), compared with model predictions of S_r using parameters calibrated directly from WRC (d).

7.3 Speswhite kaolin

Tarantino and de Col [33] studied the behaviour of Speswhite kaolin under static compaction at seven different water contents with continuous measurement of suction. The experimental results are in Fig. 9a shown in terms of S_r vs. s plots for different water contents. Figure 9b shows predictions by the proposed formulation with parameters calibrated by means of the trial-and-error procedure. The proposed state surface represents well the measured behaviour for virgin loading. As expected, the model is due to the absence of hydraulic hysteresis less successful in predicting the behaviour upon unloading-reloading cycles.

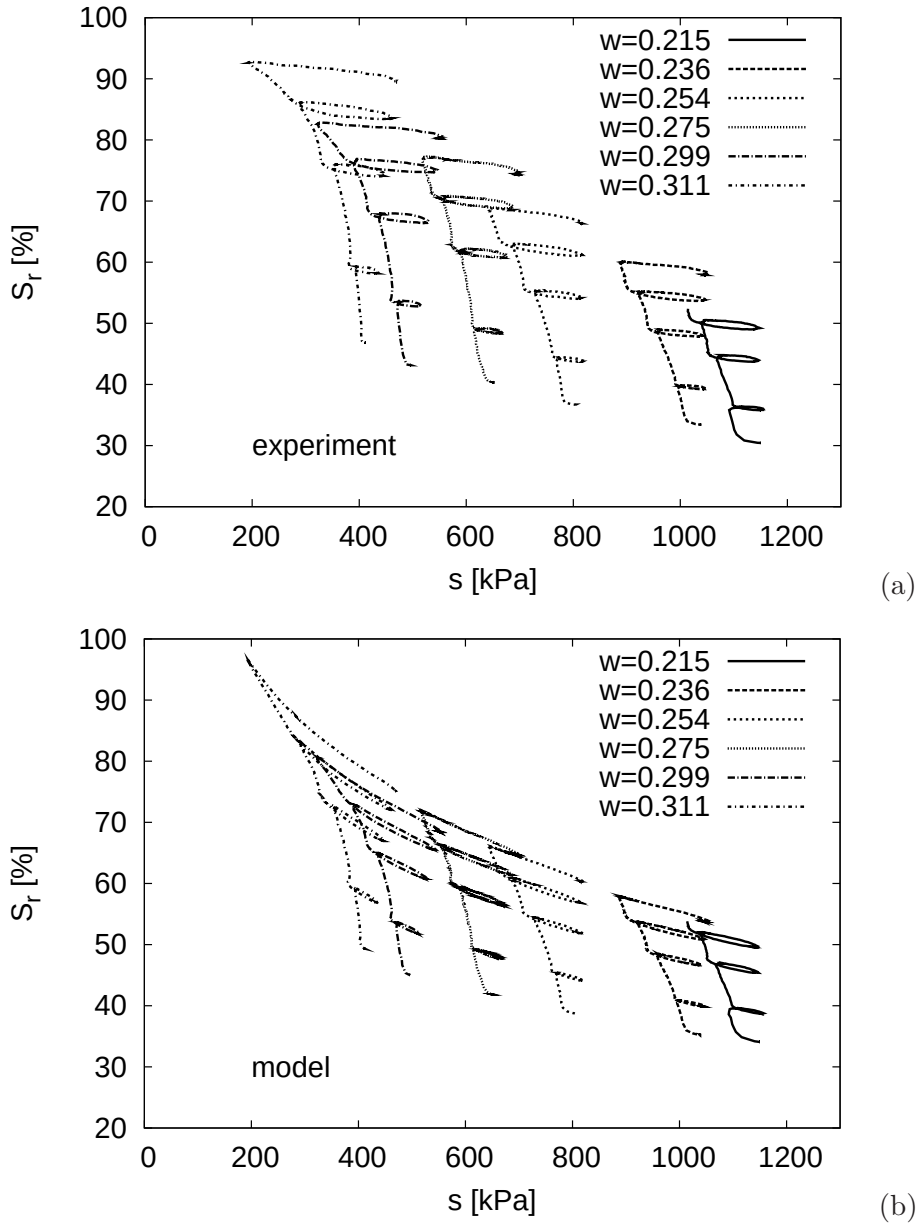

Figure 9: (a) Results of compaction tests on Speswhite kaolin by Tarantino and De Col [33] plotted in S_r vs. s graphs for constant water contents. (b) predicted results.

7.4 Bentonite/kaolin mixture

The last soil used in the evaluation is a mixture consisting of 20% bentonite and 80% kaolin, prepared by static compaction under a pressure of 400 kPa by Sharma [27]. Three samples were isotropically loaded and unloaded at constant suctions of 100, 200 and 300 kPa. Figure 10a shows dependency of void ratio on mean net stress, Figure 10b gives corresponding S_r. The model was calibrated by the trial-and-error procedure using data from Fig. 10 (see Fig. 4b for calibration using test at s=300 kPa). The obtained values $s_{e0} = 20$ kPa and $\lambda_{p0} = 0.15$ at $e_0 = 1.2$ lead to correct representation of the soil behaviour at loading/unloading at constant suction (Fig. 10c).

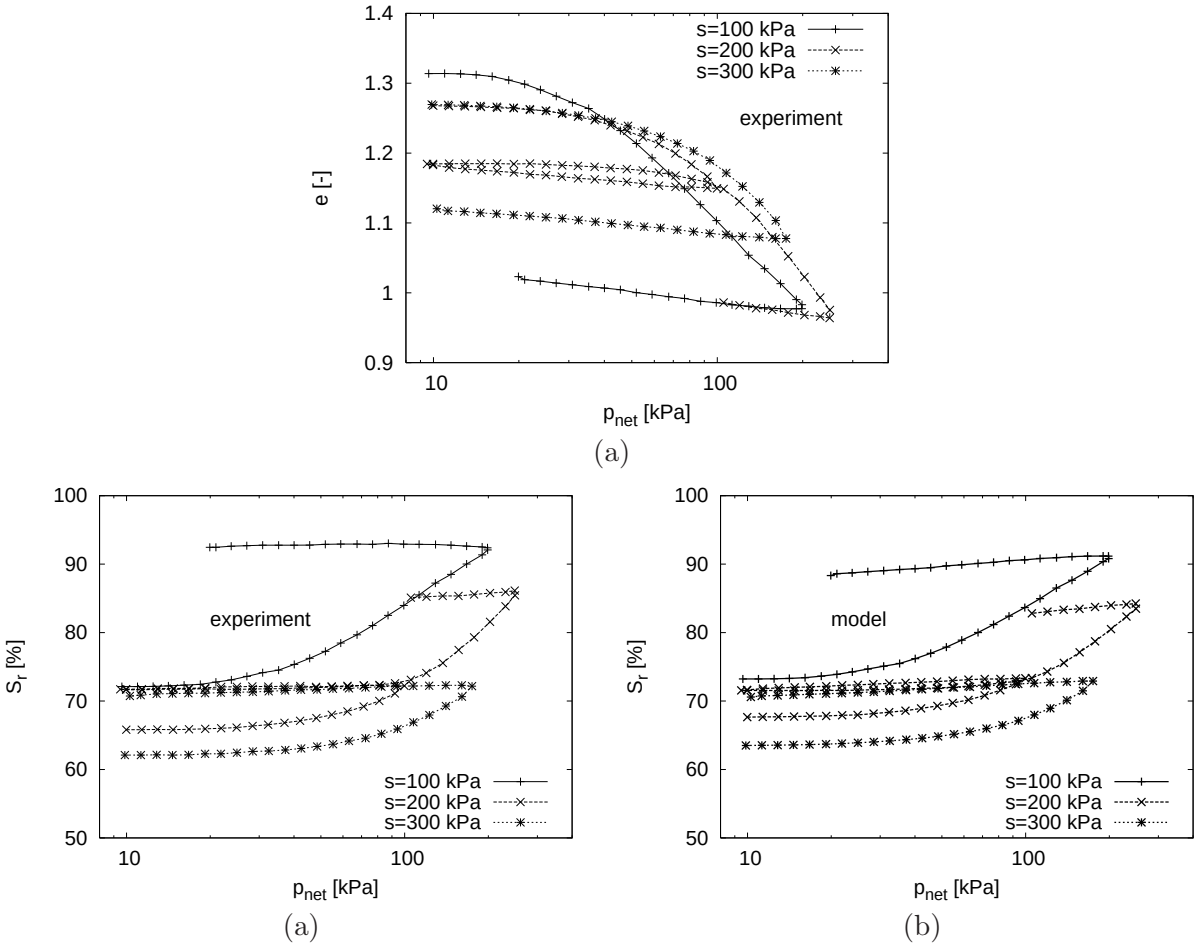

Figure 10: Experimental results of three constant suction isotropic compression tests on bentonite/kaolin mixture (a,b) by Sharma (1995), compared with model predictions of S_r (c).

The soil parameters obtained by the trial-and-error procedure using compression tests at constant suction were subsequently used to predict wetting-drying experiment on the same soil (with suction decreased from 300 kPa to 20 kPa and increased back to 300 kPa). Figure 11a shows the suction vs. void ratio relationship for this experiment, Figure 11b gives the corresponding values of S_r as measured and predicted by the model. Figure 11b shows that the model calibrated using

experiments at constant suction reproduces correctly the wetting part of the test, which proves suitability of the model to predict S_r vs. s vs. e relationship under monotonous paths. The drying path is not predicted correctly, again due to the absence of hydraulic hysteresis. It demonstrates the limitation of the present model important for applications with suction reversals.

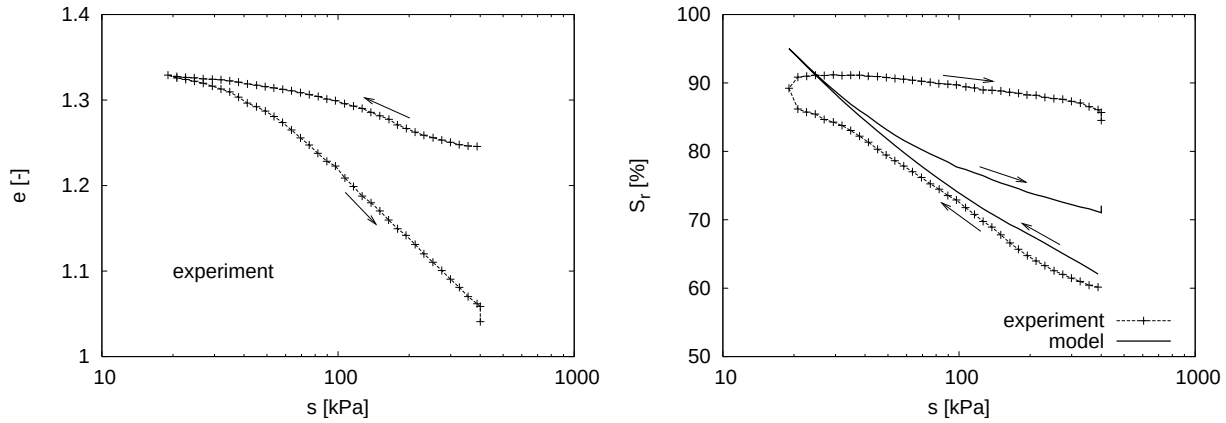

(a) (b)

Figure 11: Wetting-drying test on bentonite/kaolin mixture. Experimental results by Sharma (1995) (a,b), compared with model predictions of S_r (b), demonstrating limitation of the proposed approach for tests with suction path reversal.

8 Conclusions

Considering the existence of generalised elastic and plastic potentials defined in terms of effective stresses for unsaturated soils, Loret and Khalili [20] and Khalili et. al [14] derived a formulation relating changes of a degree of saturation to changes of void ratio and suction (Eq. (14)). Applicability of this equation for predicting changes of S_r due to variable s and e has been studied in this paper. It has been shown that when combined with a simple formulation for WRC and the effective stress formulation from [15], this equation implies void ratio dependent suction at air entry/expulsion s_e and void ratio-dependent slope λ_p of the WRC. This leads for the main wetting and drying processes to a unique state surface in the S_r vs. s vs. e space. Comparison with experimental data on several different soils showed that this surface represents well the observed soil behaviour, excluding situations where the effects of hydraulic hysteresis (not considered in the present derivations) are important. The implied dependency of WRC on void ratio may be seen as a useful enhancement of existing constitutive models for mechanical behaviour of unsaturated soils, as it does not require any additional model parameter apart from parameters specifying WRC for reference void ratio e_0. Success of Eq. (14) in predicting the

experimentally observed soil behaviour indirectly supports applicability of the effective stress principle for unsaturated soils.

9 Acknowledgement

The author wish to thank to Prof. Nasser Khalili for valuable discussions on the subject and to Dr. Alessandro Tarantino for providing experimental data on Speswhite kaolin. Financial support by the research grants GACR 205/08/0732, GACR 103/07/0678 and MSM 0021620855 is greatly appreciated.

References

[1] A. W. Bishop. The principle of effective stress. *Teknisk Ukeblad*, 106(39):859–863, 1959.

[2] G. Bolzon, A. Schrefler, and O. C. Zienkiewicz. Elasto-plastic constitutive laws generalised to partially saturated states. *Géotechnique*, 46(2):279–289, 1996.

[3] R. Brooks and A. Corey. Hydraulic properties of porous media. *Hydrology paper No. 3, Colorado state University*, 1964.

[4] M. D. Fredlund, G. W. Wilson, and D. G. Fredlund. Use of the grain-size distribution for estimation of the soil-water characteristic curve. *Canadian Geotechnical Journal*, 39:1103–1117, 2002.

[5] D. Gallipoli, A. Gens, R. Sharma, and J. Vaunat. An elasto-plastic model for unsaturated soil incorporating the effects of suction and degree of saturation on mechanical behaviour. *Géotechnique*, 53(1):123–135, 2003.

[6] D. Gallipoli, S. J. Wheeler, and M. Karstunen. Modelling the variation of degree of saturation in a deformable unsaturated soil. *Géotechnique*, 53(1):105–112, 2003.

[7] A. Gens. Constitutive modelling, application to compacted soil. In Alonso and Delage, editors, 1^{st} *Int. Conference on Unsaturated Soils, Paris, France*, volume 3, pages 1179–1200. Balkema, Rotterdam, 1996.

[8] A. Gens, M. Sánchez, and D. Sheng. On constitutive modelling of unsaturated soils. *Acta Geotechnica*, 1:137–147, 2006.

[9] G. T. Houlsby. The work input to an unsaturated granular material. *Géotechnique*, 47(1):193–196, 1997.

[10] K. Hutter, L. Laloui, and L. Vulliet. Thermodynamically based mixture models for saturated and unsaturated soils. *Mechanics of Cohesive-Frictional Materials*, 4:295–338, 1999.

[11] J. E. B. Jennings and J. B. Burland. Limitations to the use of effective stresses in saturated soils. *Géotechnique*, 12(2):125–144, 1962.

[12] A. Jotisankasa, A. Ridley, and M. Coop. Collapse behaviour of compacted silty clay in suction-monitored oedometer apparatus. *Journal of Geotechnical and Geoenvironmental Engineering*, 133(7):867–877, 2007.

[13] N. Khalili, F. Geiser, and G. E. Blight. Effective stress in unsaturated soils: review with new evidence. *International Journal of Geomechanics*, 4(2):115–126, 2004.

[14] N. Khalili, M. A. Habte, and S. Zrgarbashi. A fully coupled flow-deformation model for cyclic analysis of unsaturated soils including hydraulic and mechanical hystereses. *Computers and Geotechnics*, 35(6):872–889, 2008.

[15] N. Khalili and M. H. Khabbaz. A unique relationship for χ for the determination of the shear strength of unsaturated soils. *Géotechnique*, 48(2):1–7, 1998.

[16] L. Laloui, G. Klubertanz, and L. Vulliet. Solid-liquid-air coupling in multiphase porous media. *International Journal for Numerical and Analytical Methods in Geomechanics*, 27:183–206, 2003.

[17] R. W. Lewis and B. A. Schrefler. *The finite element method in the deformation and consolidation of porous media*. Wiley, Chichester, 1987.

[18] X. S. Li. Modelling of hysteresis response for arbitrary wetting/drying paths. *Computers and Geotechnics*, 32:133–137, 2005.

[19] A. Lloret and E. E. Alonso. State surfaces for partially saturated soils. In *Proc.* 11^{th} *Int. Conf. Soil Mechanics and Foundation Engineering, San Francisco*, pages 557–562, 1985.

[20] B. Loret and N. Khalili. A three-phase model for unsaturated soils. *International Journal for Numerical and Analytical Methods in Geomechanics*, 24:893–927, 2000.

[21] B. Loret and N. Khalili. An effective stress elastic-plastic model for unsaturated porous media. *Mechanics of Materials*, 34:97–116, 2002.

[22] E. L. Matyas and H. S. Radhakrishna. Volume change characteristics of partially saturated soils. *Géotechnique*, 18:432–448, 1968.

[23] D. Mašín and N. Khalili. A hypoplastic model for mechanical response of unsaturated soils. *International Journal for Numerical and Analytical Methods in Geomechanics*, 32(15), 2008.

[24] D. Mašín and N. Khalili. Modelling of the collapsible behaviour of unsaturated soils in hypoplasticity. In D. G. Toll, C. E. Augarde, D. Gallipoli, and S. J. Wheeler, editors, 1^{st} *European Conference on Unsaturated Soils, Durham, UK*, pages 659–665. CRC Press/Balkema, The Netherlands, 2008.

[25] M. Nuth and L. Laloui. Effective stress concept in unsaturated soils: Clarification and validation of a unified framework. *International Journal for Numerical and Analytical Methods in Geomechanics*, 32:771–801, 2008.

[26] A. R. Russell and N. Khalili. A unified bounding surface plasticity model for unsaturated soils. *International Journal for Numerical and Analytical Methods in Geomechanics*, 30(3):181–212, 2006.

[27] R. S. Sharma. *Mechanical behaviour of unsaturated highly expansive clays*. PhD thesis, University of Oxford, 1998.

[28] D. A. Sun, H. Matsuoka, and Y. F. Xu. Collapse behaviour of compacted clays in suction-controlled triaxial tests. *Geotechnical Testing Journal*, 27(4):362–370, 2004.

[29] D. A. Sun, D. Sheng, H. B. Cui, and S. W. Sloan. A density-dependent elastoplastic hydro-mechanical model for unsaturated compacted soils. *International Journal for Numerical and Analytical Methods in Geomechanics*, 31:1257–1279, 2007.

[30] D. A. Sun, D. Sheng, L. Xiang, and S. W. Sloan. Elastoplastic prediction of hydro-mechanical behaviour of unsaturated soils under undrianed conditions. *Computers and Geotechnics*, 35:845–852, 2008.

[31] D. A. Sun, D. Sheng, and Y. F. Xu. Collapse behaviour of unsaturated compacted soil with different initial densities. *Canadian Geotechnical Journal*, 44(6):673–686, 2007.

[32] R. Tamagnini. An extended Cam-clay model for unsaturated soils with hydraulic hysteresis. *Géotechnique*, 54(3):223–228, 2004.

[33] A. Tarantino and E. De Col. Compaction behaviour of clay. *Géotechnique*, 58(3):199–213, 2008.

[34] S. J. Wheeler, A. Näätänen, M. Karstunen, and M. Lojander. An anisotropic elastoplastic model for soft clays. *Canadian Geotechnical Journal*, 40:403–418, 2003.

[35] S. J. Wheeler, R. S. Sharma, and M. S. R. Buisson. Coupling of hydraulic hysteresis and stress-strain behaviour in unsaturated soils. *Géotechnique*, 53:41–54, 2003.

Appendix

This appendix describes analytical solution of Eq. (14) for unsaturated state, in which $s \geq s_e$ and $\psi = (1-\gamma)\chi$. The derivative of S_r with respect to e may be for a given suction s expressed as

$$\frac{\partial S_r}{\partial e} = \frac{\partial S_r}{\partial s_e}\frac{\partial s_e}{\partial e} + \frac{\partial S_r}{\partial \lambda_p}\frac{\partial \lambda_p}{\partial e} \tag{20}$$

which is for constant suction s according to (14) equal to $(\psi - S_r)/e$:

$$\frac{\partial S_r}{\partial e} = \frac{\psi - S_r}{e} \tag{21}$$

From Eq. (6b) follows $\partial S_r/\partial \lambda_p = S_r \ln(s_e/s)$ and $\partial S_r/\partial s_e = \lambda_p S_r/s_e$. We therefore have

$$\frac{\psi - S_r}{e} = \frac{\partial \lambda_p}{\partial e} S_r \ln\left(\frac{s_e}{s}\right) + \frac{\partial s_e}{\partial e}\left(\frac{\lambda_p S_r}{s_e}\right) \tag{22}$$

At transition between unsaturated and saturated states we have $s = s_e$ and $S_r = \chi = 1$. Eq. (22) then simplifies to the following rate equation for s_e:

$$\dot{s}_e = -\frac{\gamma s_e}{e\lambda_{psu}}\dot{e} \tag{23}$$

where λ_{psu} is the value of λ_p corresponding to the transition between saturated and unsaturated states, i.e. to $s = s_e$. As will be shown further, the value of λ_p does not depend significantly on

suction. We may therefore assume $\lambda_{psu}/\lambda_p = 1$. Substitution of (23) into (22) then yields

$$\frac{\psi - S_r}{e} = -\frac{\gamma S_r}{e} + S_r \ln\left(\frac{s_e}{s}\right) \frac{\partial \lambda_p}{\partial e} \tag{24}$$

from which follows the partial derivative of λ_p with respect to e:

$$\frac{\partial \lambda_p}{\partial e} = \frac{(1-\gamma)(\chi - S_r)}{e S_r \ln\left(\frac{s_e}{s}\right)} \tag{25}$$

after substitution of $\chi = (s_e/s)^\gamma$ and $S_r = (s_e/s)^{\lambda_p}$ we have

$$\frac{\partial \lambda_p}{\partial e} = \frac{(1-\gamma)\left[\left(\frac{s_e}{s}\right)^\gamma - \left(\frac{s_e}{s}\right)^{\lambda_p}\right]}{e\left(\frac{s_e}{s}\right)^{\lambda_p} \ln\left(\frac{s_e}{s}\right)} \tag{26}$$

Thanks to the minor dependency of λ_p on suction, we may substitute s_e/s by s_{e0}/s:

$$\frac{\partial \lambda_p}{\partial e} = \frac{(1-\gamma)\left(\chi_0 - \left(\frac{s_{e0}}{s}\right)^{\lambda_p}\right)}{e\left(\frac{s_{e0}}{s}\right)^{\lambda_p} \ln\left(\frac{s_{e0}}{s}\right)} \tag{27}$$

where $\chi_0 = (s_{e0}/s)^\gamma$. Therefore

$$\int_{e0}^{e} \frac{de}{e} = \frac{\ln\left(\frac{s_{e0}}{s}\right)}{\chi_0(1-\gamma)} \int_{\lambda_{p0}}^{\lambda_p} \left[\frac{\left(\frac{s_{e0}}{s}\right)^{\lambda_p}}{\left(1 - \frac{1}{\chi_0}\left(\frac{s_{e0}}{s}\right)^{\lambda_p}\right)}\right] d\lambda_p \tag{28}$$

The right-hand side of Eq. (28) may be solved by considering

$$\int \frac{c^x}{1 + bc^x} dx = \frac{1}{b \ln c} \ln\left(bc^x + 1\right) + C \tag{29}$$

with $x = \lambda_p$, $c = s_{e0}/s$ and $b = -1/\chi_0$. We therefore have

$$\ln e = \frac{1}{\gamma - 1}\left(\ln\left[\chi_0 - \left(\frac{s_{e0}}{s}\right)^{\lambda_p}\right] - \ln \chi_0\right) + C \tag{30}$$

After substituting the integration bounds e_0 and λ_{p0} and some manipulation we finally obtain

$$\lambda_p = \frac{\gamma}{\ln \chi_0} \ln\left[\left(\chi_0^{\frac{\lambda_{p0}}{\gamma}} - \chi_0\right)\left(\frac{e}{e_0}\right)^{(\gamma-1)} + \chi_0\right] \tag{31}$$

λ_{psu} from Eq. (23) is obtained from Eq. (31) by setting $s = s_e$, i.e.

$$\lambda_{psu} = \frac{\gamma}{\ln \chi_{0su}} \ln \left[\left(\chi_{0su}^{\frac{\lambda_{p0}}{\gamma}} - \chi_{0su} \right) \left(\frac{e}{e_0} \right)^{(\gamma-1)} + \chi_{0su} \right] \tag{32}$$

with $\chi_{0su} = (s_{e0}/s_e)^{\gamma}$.

To demonstrate that the simplifications introduced (neglecting the dependency of λ_p on suction in Eqs. (24) and (27)) has minor influence on calculated results, Fig. 12a shows λ_p values calculated according to Eq. (31) ("approximate solution") compared with λ_p values obtained by numerical integration of Eq. (21) ("exact solution") for different suctions and void ratios. The results practically coincide; in terms of S_r (Fig. 12b) they may be considered as equal.

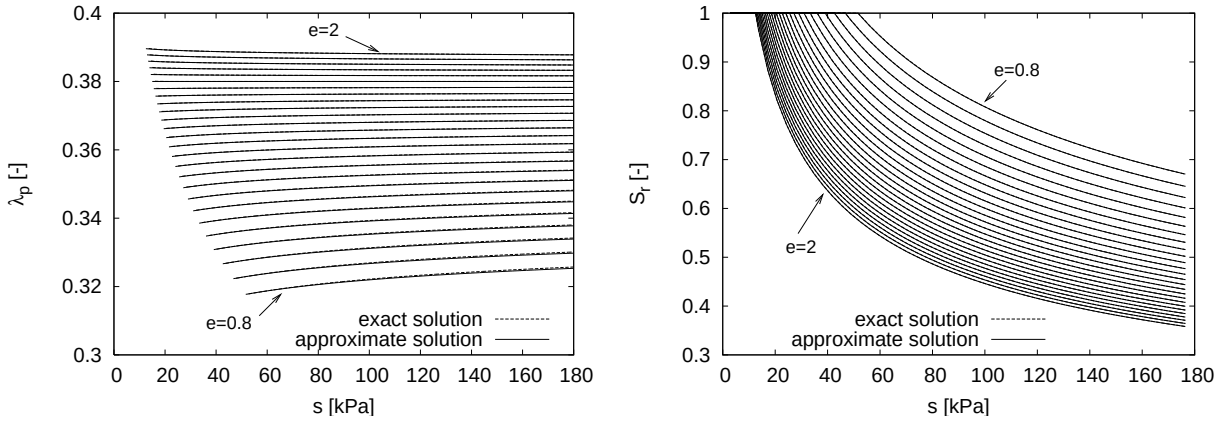

Figure 12: Comparison of exact and approximate solutions of Eq. (21).

List of Figures

List of Tables